

1 **Title: Neural dynamics of real-world object vision that guide**
2 **behaviour**

3
4 Radoslaw M. Cichy¹, Nikolaus Kriegeskorte², Kamila M. Jozwik¹, Jasper J.F. van den Bosch², Ian
5 Charest³

6
7 ¹ Department of Education and Psychology, Free University Berlin, Berlin, Germany

8 ² MRC Cognition and Brain Sciences Unit, University of Cambridge, Cambridge, UK

9 ³ School of Psychology, University of Birmingham, Birmingham, UK

10

11

12

13

14

15

16

17

18

19 **CORRESPONDING AUTHOR**

20 Radoslaw Martin Cichy

21 Department of Education and Psychology

22 Free University Berlin

23 JK 25/221b

24 Berlin, Germany

25 Phone: +49 40 838 61132

26 Email: radoslaw.cichy@fu-berlin.de

27

28

29 **KEYWORDS**

30 object recognition, MEG, fMRI, representational similarity analysis

31 **1 Abstract**

32 Vision involves complex neuronal dynamics that link the sensory stream to behaviour. To
33 capture the richness and complexity of the visual world and the behaviour it entails, we used an
34 ecologically valid task with a rich set of real-world object images. We investigated how human
35 brain activity, resolved in space with functional MRI and in time with magnetoencephalography,
36 links the sensory stream to behavioural responses. We found that behaviour-related brain
37 activity emerged rapidly in the ventral visual pathway within 200ms of stimulus onset. The link
38 between stimuli, brain activity, and behaviour could not be accounted for by either category
39 membership or visual features (as provided by an artificial deep neural network model). Our
40 results identify behaviourally-relevant brain activity during object vision, and suggest that
41 object representations guiding behaviour are complex and can neither be explained by visual
42 features or semantic categories alone. Our findings support the view that visual representations
43 in the ventral visual stream need to be understood in terms of their relevance to behaviour,
44 and highlight the importance of complex behavioural assessment for human brain mapping.

45 **2 Introduction**

46 To survive, visual animals must form accurate representations of the world to guide behaviour
47 (Heekeren et al., 2008; Panzeri et al., 2017). The underlying neural mechanisms can be
48 formalized as a two-step mapping from sensory input to neural representations, and from
49 neural representations to behaviour. While each of the two steps can in principle be
50 investigated in separation, as visual recognition (DiCarlo et al., 2012) and perceptual decision
51 making (Heekeren et al., 2008), only a combined investigation of both steps can demonstrate
52 that experimentally measured activity during perception is in fact used by the brain to guide
53 behaviour (de-Wit et al., 2016; Panzeri et al., 2017).

54
55 Most previous research has employed one of two strategies to investigate the triadic
56 relationship between sensory input, neural representation and behaviour. The first approach is
57 to relate human performance in binary classification tasks to brain activity (Newsome et al.,
58 1989; Britten et al., 1996; Thorpe et al., 1996; Grill-Spector et al., 2000; VanRullen and Thorpe,
59 2001; Philiastides and Sajda, 2006; Williams et al., 2007; Ratcliff et al., 2009; Carlson et al.,
60 2013; Ritchie et al., 2015). This strategy is experimentally elegant in its simplicity and of direct
61 relevance to categorisation as a major function of the human visual system. However, it does
62 not address the complexity and richness of human visual experience: our perception of the
63 world is not binary but it is organised according to many properties, such as shape, colour and
64 category.

65
66 A second strategy is to establish a second-order similarity between behavioural judgments and
67 neural activity. If two stimuli with similar neural representations are judged as being similar
68 perceptually, this suggests a role of the neural representations in guiding behaviour. This
69 approach has established a role for the behavioural relevance of object shape representations
70 in primate brains focusing mostly on artificial shape stimuli (Op de Beeck et al., 2001; Kayaert et
71 al., 2005; Haushofer et al., 2008; Op de Beeck et al., 2008b p.200; Walther et al., 2009).
72 However, it is unclear how the link between neural representations and behavior holds in a
73 more ecologically valid setting with a large set of real-world stimuli.

74
75 Here, by combining elements of both strategies we epitomized on their respective advantages.
76 First, to assess human behaviour related to perception of real-world visual objects, we assessed
77 behaviour using a similarity judgments task where multiple object-pair similarities are judged at
78 once (Kriegeskorte and Mur, 2012) for a large set of objects, establishing the link between
79 visual input and behaviour. Second, we resolved brain responses to the same visual stimuli in
80 space by full-brain functional magnetic resonance imaging (fMRI) and in time by
81 magnetoencephalography (MEG), establishing the link between experimental stimuli and brain
82 activity. Third, using representational similarity analysis (RSA; Kriegeskorte and Kievit, 2013), we

83 forged a link between perceptual judgments and brain activity, resolving behaviour-relevant
84 brain activity during object vision in both space and time.

85 **3 Materials and Methods**

86 **3.1 Visual stimulus set and experimental design**

87 The stimulus set consisted of 118 square images of everyday objects, each one from a different
88 category, on real-world backgrounds from the ImageNet database (Fig. 1A). The same stimulus
89 set was used in three separate experiments: behavioural, MEG and fMRI. The experiments were
90 conducted according to the Declaration of Helsinki and approved by the respective local ethics
91 committees (for fMRI and MEG experiments: Institutional Review Board of the Massachusetts
92 Institute of Technology, for behavioural experiments: Ethics Committee of the Free University
93 Berlin).

94 **3.2 Behavioural ratings of perceived similarity**

95 Participants ($n = 20$, 11 female, age: mean \pm s.d. = 25.47 \pm 7.09 years) gave ratings on the
96 perceived similarity of object images in a multiple arrangements task (Kriegeskorte and Mur,
97 2012; Charest et al., 2014). Participants were asked to arrange the images on a computer
98 screen inside a white circular arena by using computer mouse drag and drop operations. On the
99 first trial, the participants arranged all the images at once, and subsequent trials were
100 constructed with an adaptive selection procedure, optimizing information for all possible pairs
101 of images. These subsequent trials often included items that were placed close together in the
102 initial trial (sometimes in small piles). As subsequent trials included fewer objects to place,
103 participants could refine their judgements with distinctions that are more difficult to carry in
104 the context of the whole image set and the limited arena space. This task is efficient when
105 dealing with large number of stimuli, and reliable similarity judgments were obtained with 60
106 minutes of total experiment time per participant.

107 **3.3 Neuroimaging experiments: participants and experimental design**

108 MEG and fMRI data have been published previously (Cichy et al., 2016b). Here we provide a
109 summary of the relevant parameters.

110

111 Participants ($n = 15$, 5 female, age: mean \pm s.d. = 26.6 \pm 5.18 years) took part in an fMRI and
112 MEG experiment. These participants were distinct from the participants that took part in the
113 behavioural experiment. All participants were healthy and right handed with normal or
114 corrected-to-normal vision. The stimulus set was identical to the one in the behavioural
115 experiment. In both the fMRI and MEG experiments, images were presented at the center of a
116 screen at 4.0° visual angle with 500 ms duration, overlaid with a gray fixation cross. Further

117 presentation parameters were adjusted to the specific requirements of each imaging
118 technique.

119

120 In the MEG experiment, each participant completed one session consisting of 15 runs of 314 s
121 duration each. In each run, every object image was shown twice, with random condition order
122 and a trial onset asynchrony of 0.9-1 s. Participants were instructed to respond to the image of
123 a paper clip shown randomly every 3-5 trials (average 4) with an eye blink and a button press,
124 and not to blink their eyes at other times.

125

126 In the fMRI experiment, each participant completed two sessions of 9-11 runs of 486 s duration
127 each. In each run, every object image was shown once, and condition order was randomized
128 with an inter-trial interval of 3s. In addition, 39 null trials (gray background) were interspersed
129 randomly during which only a gray background was presented. Participants were instructed to
130 respond to the change in luminance of the fixation cross with a button press.

131 **3.4 MEG acquisition and preprocessing**

132 MEG signals were recorded with a sampling rate of 1 kHz, filtered between 0.03 and 330 Hz,
133 from 306 channels (204 planar gradiometers, 102 magnetometers, Elekta Neuromag TRIUX,
134 Elekta, Stockholm). We applied temporal source space separation (maxfilter software, Elekta,
135 Stockholm (Taulu et al., 2004; Taulu and Simola, 2006)) before analysing data with the
136 Brainstorm software (Tadel et al., 2011). We epoched data from -100ms to +700ms with
137 respect to the onset of each trial, removed baseline mean and smoothed data with a 20-ms
138 sliding window. This resulted in 30 trials for each condition, session, and participant.

139

140 To determine the time-resolved similarity relations between visual representations revealed by
141 MEG, we used multivariate pattern analysis as described previously (Cichy et al., 2014, 2016b).
142 The rationale is that the more dissimilar two visual representations are, the more dissimilar are
143 the resulting MEG channel activation patterns, and the better is the performance of the
144 classifier. Thus, classifier performance can be interpreted as a dissimilarity measure of neural
145 representations. We analysed data separately for each subject. For each time point, we
146 extracted and arranged MEG data as 306 dimensional measurement vectors (corresponding to
147 the 306 MEG sensors), yielding 30 raw pattern vectors per condition. We averaged raw pattern
148 vectors by 5 before multivariate analysis to reduce computational load. We used supervised
149 learning with a leave-one-trial-out cross-validation scheme to train and test a support vector
150 machine (SVM) to discriminate each pair of conditions in the LibSVM implementation
151 (<http://www.csie.ntu.edu.tw/~cjlin/libsvm>). Each pairwise discrimination was repeated 100
152 times with random assignment of raw trials to average trials, and average trials to the training
153 and testing set. Resulting decoding accuracies were averaged across cross-validation iterations,

154 and assigned to a matrix of size 118×118 , with rows and columns indexed by the classified
155 conditions. The matrix was symmetric and the diagonal was undefined. This procedure yielded
156 one 118×118 matrix of decoding accuracies for every time-point, and we refer to it as the MEG
157 representational dissimilarity matrix (MEG RDM).

158 **3.5 fMRI acquisition & analysis**

159 We acquired MRI data on a 3T Trio scanner (Siemens, Erlangen, Germany) with a 32-channel
160 head coil. Structural images were acquired using a standard T1-weighted sequence (192 sagittal
161 slices, FOV = 256 mm^2 , TR = 1,900 ms, TE = 2.52 ms, flip angle = 9°). Functional images covering
162 the whole cortex were acquired in runs of 648 volumes using a gradient-echo EPI sequence (TR
163 = 750 ms, TE = 30 ms, flip angle = 61° , FOV read = 192 mm, FOV phase = 100% with a partial
164 fraction of 6/8, through-plane acceleration factor 3, bandwidth 1816Hz/Px, resolution = 3mm^3 ,
165 slice gap 20%, slices = 33, ascending acquisition).

166
167 We processed fMRI data using SPM8 (<http://www.fil.ion.ucl.ac.uk/spm/>) for each participant
168 separately. We realigned and co-registered fMRI data to the T1 structural scan before
169 normalizing it to the standard MNI template. To estimate condition-specific responses, we used
170 a general linear model (GLM) into which image onsets were entered as regressors and were
171 convolved with a hemodynamic response function. We included movement parameters as
172 nuisance regressors. The estimated condition-specific GLM parameters were converted into t -
173 values by contrasting each condition estimate against the implicitly modelled baseline.

174
175 To determine the spatial dynamics of object vision, and to relate them to behaviour, we
176 analysed fMRI data using a spatially unbiased searchlight approach (Kriegeskorte et al., 2006;
177 Haynes et al., 2007). In detail, for each voxel v , we extracted condition-specific t -value patterns
178 in a sphere centred at v with a radius of 4 voxels (searchlight at v) and arranged them into
179 pattern vectors. For each pair of conditions, we calculated the dissimilarity between pattern
180 vectors by 1 minus Spearman's ρ , resulting in 118×118 fMRI representational dissimilarity
181 matrices (fMRI RDM) indexed in columns and rows by the compared conditions. fMRI RDMs
182 were symmetric across the diagonal, and entries were bounded between 0 (no dissimilarity)
183 and 2 (complete dissimilarity). This procedure resulted in one fMRI RDM for each voxel in the
184 brain.

185 **3.6 Representational similarity analysis between behaviour RDMs and neuroimaging** 186 **data**

187 To identify behaviour-relevant brain dynamics in space and in time, we related behavioural
188 ratings to brain activity using representational similarity analysis (RSA).

189

190 To investigate temporal dynamics, we conducted time-resolved RSA between the behaviour
191 RDM and MEG RDMs. For each subject separately, and for each time point, we correlated the
192 time-point specific RDM with the average behaviour RDM. This resulted in a behaviour-MEG
193 representational time course for each subject.

194

195 To investigate spatial dynamics, we conducted spatially-resolved RSA between behaviour RDM
196 and fMRI RDMs. For this we used a searchlight analysis (Haynes and Rees, 2005a; Kriegeskorte
197 et al., 2006). For each voxel we correlated (Spearman's ρ) the fMRI RDM with the behaviour
198 RDM, and saved the correlation coefficient at the position of the voxel. This resulted in a 3D
199 representational similarity map for each participant.

200 **3.7 Assessing the role of categories and visual features**

201 To investigate the nature of the representational relations captured by RSA between
202 neuroimaging data and behaviour, we conducted two additional analyses.

203

204 First, we investigated the level of categorical abstraction at which similarities between the brain
205 and behaviour emerged. While the stimulus set was designed such that every object was from a
206 different entry-level category, multiple objects fell into supra-level categories. Thus, putative
207 representational similarities between brain and behaviour might be explained at the level of
208 supra-categories, rather than categories. We identified the following supra-level categories in
209 the stimulus set, guided by semantic divisions in the organisation of object knowledge in the
210 human brain observed in neuropsychological research (Warrington and Shallice, 1984; Hart et
211 al., 1985; Damasio, 1990; Martin et al., 1996; Caramazza and Mahon, 2003; Mahon and
212 Caramazza, 2009). Two subjects performed category classification with the following results:
213 animate objects (27), and inanimate objects (91), where animate are further subdivided into
214 tools (21), food (18), music instruments (9), means of transport (9), electric appliance (11), balls
215 (6), furniture (4) and miscellaneous (14). To assess the effect of supra-category, for each of the
216 9 subdivisions, we defined three model RDMs that capture the mean effects within each
217 subdivision (e.g. for animate: within animate, within non-animate, and between animate &
218 inanimate). Model RDMs were set to 1 for matrix elements defined by the relevant subdivision
219 (e.g. for within animate: all matrix elements defined by animate objects, or between animate &
220 inanimate: all matrix elements defined by comparison of animate & inanimate objects), and 0
221 otherwise. In total, this resulted in 27 model RDMs. We then used partial correlation analysis in
222 the fMRI and MEG-to-behaviour RSA analysis, partialling out the effect of those 27 RDMs, and
223 thus the effect of supra-category.

224

225 Second, we investigated whether visual features can account for the observed behaviour-brain
226 correspondence. To characterize images by visual features, we used deep neural networks

227 (DNN) trained on object categorisation. This model class has been shown to perform best on
228 object categorisation tasks (Krizhevsky et al., 2012; He et al., 2015), and to predict visual object-
229 related brain activity better than any previous model class (Khaligh-Razavi and Kriegeskorte,
230 2014; Yamins et al., 2014; Güçlü and Gerven, 2015; Cichy et al., 2016a). We constructed RDMs
231 based on DNN layer-specific activation patterns of the stimulus set from an 8-layer artificial
232 DNN trained on object categorisation on 683 object categories (for details see: (Cichy et al.,
233 2016a), network available here: http://brainmodels.csail.mit.edu/object_dnn.tar.gz). We then
234 used partial correlation analysis in the fMRI and MEG-to-behaviour RSA analysis, partialling out
235 the effect of those 8 DNN RDMs.

236 **3.8 Identification of behaviourally-relevant aspects of spatio-temporally resolved** 237 **neural dynamics**

238 We combined MEG and fMRI using representational similarity fusion to resolve brain dynamics
239 related to behaviour in space and time simultaneously (Cichy et al., 2016b; Cichy and Teng,
240 2017). The rationale is that if signals in the MEG originate from locations resolved in fMRI, their
241 RDMs should be similar. In addition, identifying the subset of such time point-location RDMs
242 pairs, that also correspond to the behaviour RDMs, identifies the behaviourally relevant subset
243 of brain activity. We performed a searchlight analysis for each fMRI subject ($n = 15$) and each
244 time point from 0 to +500 ms in 5 ms steps. For each voxel, we correlated (Spearman's ρ) the
245 searchlight-specific fMRI RDM and the subject-averaged MEG RDMs. Repeated for every voxel
246 in the brain this resulted in a 3D map of representational similarity between fMRI and MEG at a
247 particular time point. When repeated for all time points, this resulted in a series of 3D maps
248 revealing the spatio-temporal activation of the human brain during object perception as
249 measured with MEG and fMRI respectively. In order to identify behaviourally-relevant aspects,
250 we masked the results in space and time by the results of the MEG-behaviour and fMRI-
251 behaviour RSA.

252 **3.9 Statistical testing**

253 We conducted non-parametric random effects statistics for all tests. In detail, we used right-
254 sided sign-rank tests and corrected for multiple comparisons by FDR ($p < 0.05$) correction. We
255 used bootstrapping of the participant pool (10,000 iterations) to determine 95% confidence
256 intervals on MEG-behaviour RSA peak latencies.

257 **4 Results**

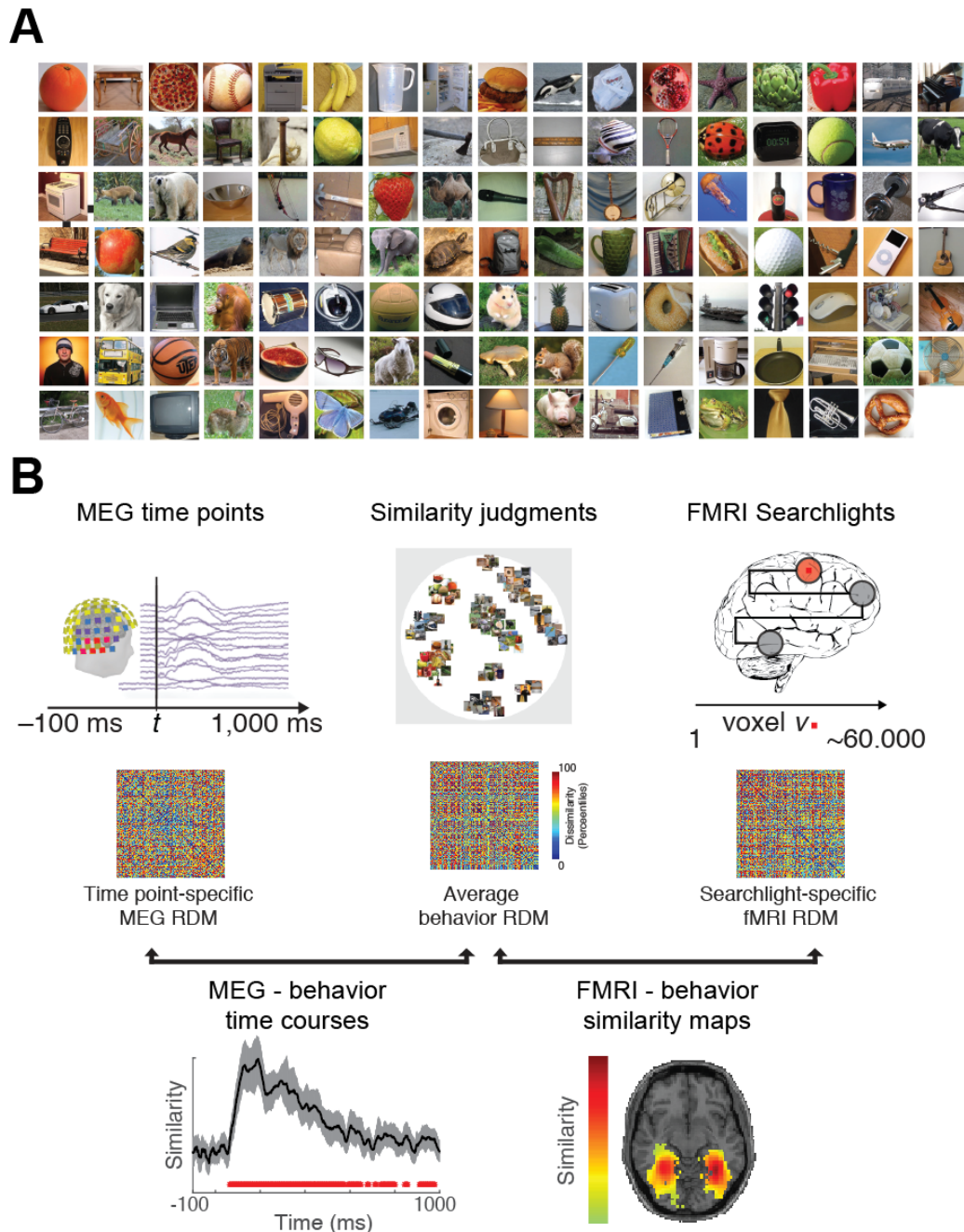
258 In order to investigate the triadic relationship between sensory stimuli, neural representations
259 and behaviour, we acquired behavioural and neural measures for a set of 118 real-world object
260 stimuli (Fig. 1A). As a measure of behaviour, participants ($N=20$) completed a perceptual
261 similarity judgment task. Participants arranged object images by their similarity in a 2D arena

262 (Kriegeskorte and Mur, 2012). To assess neural activity with both high spatial and temporal
263 resolution, we acquired full-brain fMRI and MEG measurements while participants were
264 presented with the object images.

265

266 We related the data from MEG, fMRI and similarity judgments using RSA (Kriegeskorte, 2008;
267 Kriegeskorte and Kievit, 2013) (Fig. 1B). In short, we computed representational dissimilarity
268 matrices (RDMs) that capture the representational geometry between stimulus specific signals
269 in their respective source spaces (i.e. behaviour RDMs, MEG RDMs, and fMRI RDMs). To reveal
270 the temporal dynamics of behaviourally-relevant brain activity we compared the behaviour
271 RDM to the time-resolved MEG RDMs (Carlson et al., 2012; Cichy et al., 2014). To identify the
272 locus of behaviourally-relevant aspects of neural activity during object vision, we compared the
273 behaviour RDMs to fMRI RDMs in a searchlight procedure (Haynes and Rees, 2005b;
274 Kriegeskorte et al., 2006).

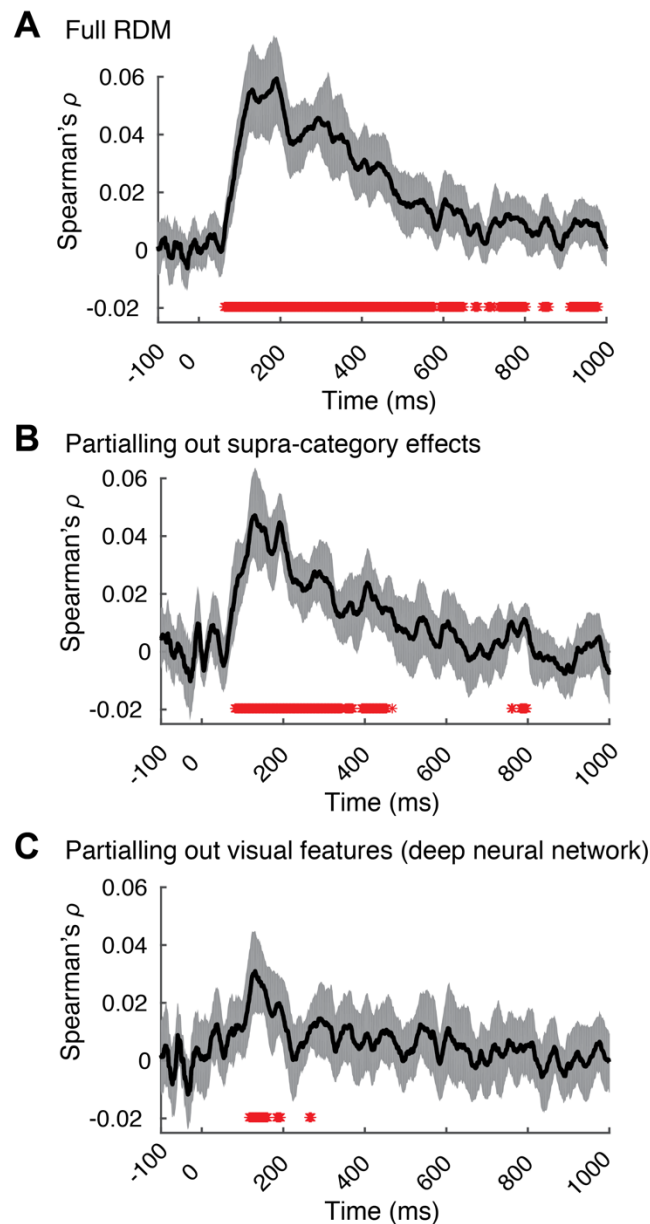
275



276

277 *Figure 1: Stimulus set and analysis rationale. A) The stimulus set consisted of 118 images of real-world objects, each from a*
 278 *different basic level category. B) General analysis rationale. We used representational similarity analysis to link sensory input,*
 279 *neural activity and behaviour related to visual objects together in a common quantitative framework. We assessed behaviour*
 280 *using a similarity-based multiple arrangements task, and summarized the results in a behaviour RDM. To resolve the temporal*
 281 *aspects of behaviour-relevant brain activity, we compared the behaviour RDM with MEG RDMs in a time resolved fashion, from -*
 282 *100 to +1000ms with respect to image onset. To resolve behaviour-relevant brain activity in space, we compared the behaviour*
 283 *RDM with fMRI RDMs in a searchlight procedure, yielding a 3D map of representational similarity between behaviour and neural*
 284 *patterns. This analysis yielded time courses of representational similarity between behaviour and neural dynamics.*

285 **4.1 The temporal dynamics of behaviourally-relevant brain activity in object vision**
286



287
288 *Figure 2: Temporal dynamics of behaviour-relevant brain activity. A) Representational similarity analysis revealed a rapid*
289 *emergence of a positive correlation between perceptual similarity judgments and brain representations. A partial correlation*
290 *analysis revealed that neither B) supra-category membership, nor C) visual features as assessed by a deep neural network*
291 *fully explained the behaviour-brain relationship.*

292 To investigate how behaviourally-relevant brain activity during object vision emerges over time,
293 we correlated the average behaviour RDM with MEG RDMs (N=16) from -100 to +1,000 ms in 1
294 ms steps with respect to stimulus onset (Fig. 1B). We found that the time course peaked at 191
295 ms (122 – 197 ms) (Fig. 2A), followed by a gradual decline. This demonstrates that brain activity

296 relevant for complex behaviour emerges rapidly in the human brain, providing the basis for fast
297 responses to the environment.

298

299 Previous research has suggested two prominent explanations for the link between neural
300 activity and visual behaviour. The first line of research has highlighted the role of category
301 membership in brain and behaviour. Stimuli that belong to different categories evoke different
302 brain responses and are judged as different (Rosch et al., 1976; Caramazza and Mahon, 2003;
303 Grill-Spector and Malach, 2004; Op de Beeck et al., 2008a). The second line of research has put
304 forward the importance of visual features (Tanaka, 1996; Op de Beeck et al., 2008a; Yamins et
305 al., 2014). According to this idea, stimuli that are characterised by different visual features
306 evoke different brain responses and are judged as different.

307 We performed control analyses to investigate the importance of category-membership and
308 visual features for the emergence of the link between brain and behaviour. Concerning
309 categories, any sizeable number of natural objects will ultimately be classified in super-ordinate
310 groupings. Our stimulus set consisted of several supra-level categorical divisions: animals (27),
311 tools (21), food (18), music instruments (9), means of transport (9), electric appliances (11),
312 balls (6), furniture (4) and miscellaneous (14). To investigate the role of category-membership
313 in the brain-behaviour relationship, we repeated our MEG-to-behaviour similarity analysis while
314 partialling out the effect of putative differences due to supra-level category membership. This
315 analysis revealed a significant effect with a peak at 130 ms (122 – 196 ms) (Fig. 2B), indicating
316 that supra-category membership is not the only factor driving the brain-behaviour relationship.

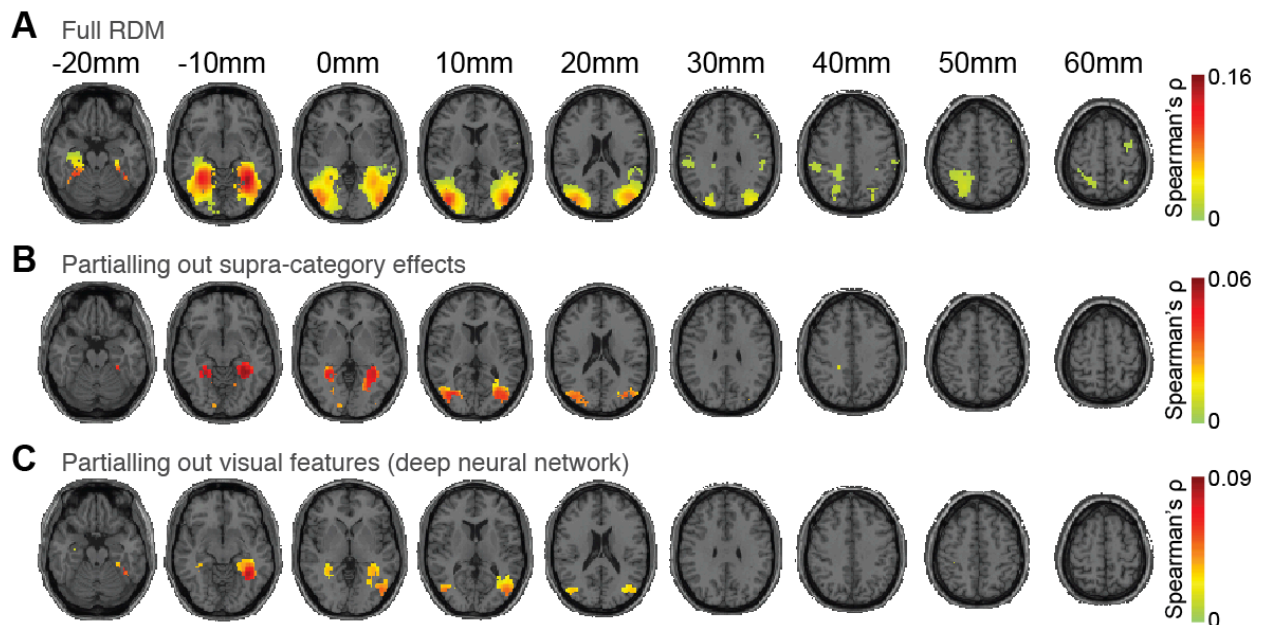
317

318 To investigate the role of visual features in the brain-behaviour relationship, we used an
319 artificial deep neural network (DNN) trained to classify objects as a proxy for these objects'
320 visual features. DNNs have been shown to explain visual representations in the brain better
321 than any other previous models (Khaligh-Razavi and Kriegeskorte, 2014; Yamins et al., 2014;
322 Güçlü and Gerven, 2015; Cichy et al., 2016a), and to predict human behaviour considerably well
323 (Khosla et al., 2015; Kubilius et al., 2016; Peterson et al., 2016). To investigate the role of visual
324 features, we repeated the MEG-to-behaviour analysis while partialling out the effect of DNN
325 visual features. This revealed a significant effect with a peak at 131 ms (123 – 568 ms) (Fig 3C),
326 demonstrating that the link between brain activity and behaviour cannot be fully explained by
327 visual features from DNNs.

328

329 Together, these results indicate that the emergence of behaviourally-relevant aspects of object
330 representations is rapid, and neither fully explained by supra-ordinate categorisation, nor by
331 visual features.

332 4.2 The spatial dynamics of behaviourally-relevant brain activity in object vision



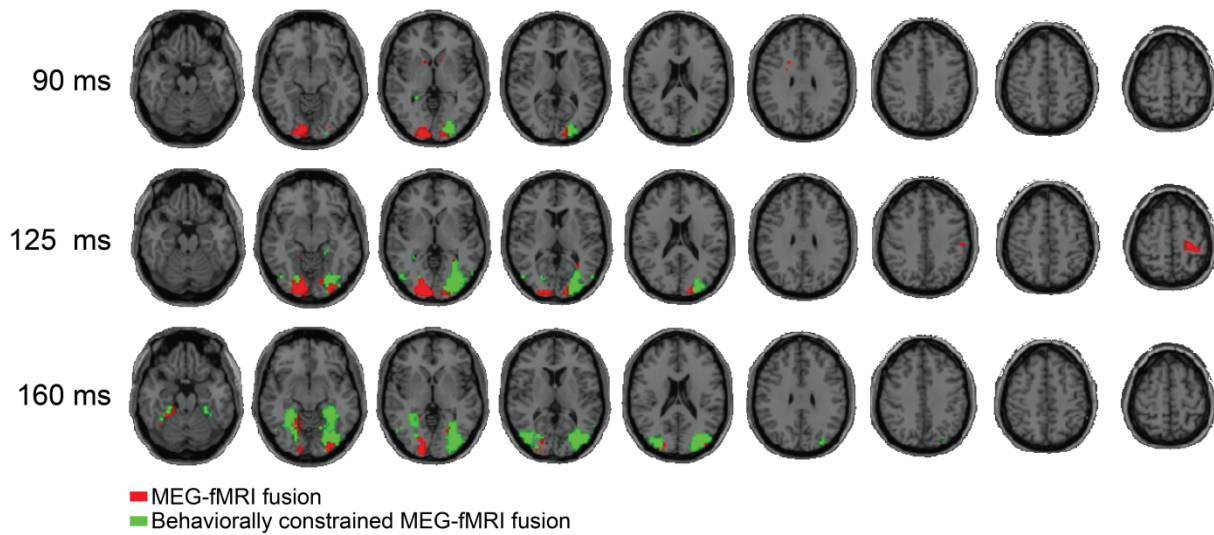
333
334 *Figure 3: Spatial dynamics of behaviour-relevant brain activity. A) Searchlight-based representational similarity analysis*
335 *revealed a positive correlation between perceptual similarity judgments and brain representations with highest correlation in*
336 *high-level ventral visual cortex. A partial correlation analysis revealed that neither B) supra-category membership, nor C) visual*
337 *features discovered by a deep neural network trained on object categorisation fully explained the behaviour-brain relationship.*

338
339 We then investigated the role of category membership and visual features in the spatially
340 resolved brain-behaviour relationship. Neither partialling out the effects of supra-level category
341 membership (Fig. 3B), nor the visual features (Fig. 3C) abolished the significant brain-to-
342 behaviour relationship in high-level ventral visual cortex.

343
344 Together, these results link behaviour to object representations in high level visual cortex and
345 show that neither category membership nor visual feature similarity can fully account for this
346 link.

347

348 4.3 Integrating spatial and temporal aspects of behaviour-relevant brain activity



349

350 *Figure 4: Spatio-temporally resolved behaviour-relevant brain activity during object vision. We used representational-similarity-*
351 *based MEG-fMRI fusion ($N = 16$, $p < 0.05$, FDR-corrected) to identify the spatio-temporal dynamics of brain activity during object*
352 *vision. Red voxels indicate the significant spatio-temporal maps reflecting MEG-fMRI correspondence. Green voxels indicate the*
353 *behaviourally-relevant subset of those maps, identified by masking the results of the MEG-fMRI fusion with time points and*
354 *locations identified as behaviourally relevant in the analyses relating MEG and fMRI to behavioural similarity ratings separately.*
355 *For a fully temporally resolved view see Movie 1.*

356 The aforementioned analyses revealed that behaviour-relevant brain activity was present over
357 a long period of time and in several brain regions. These findings raise the question of how
358 brain regions map onto temporal processing stages: at which time point is which region of the
359 brain the source of behaviour-relevant brain activity? To resolve the many-to-many mapping
360 between MEG time points and brain regions, we used RSA based MEG-fMRI fusion (Cichy et al.,
361 2014, 2016b). This approach allows identifying the spatio-temporal components of brain
362 activity during object vision that guide behaviour (Philiastides and Sajda, 2007; Cichy et al.,
363 2016b). First, we computed the representational similarity between fMRI locations and MEG
364 time points ($N = 15$, right-sided signed-rank test, $p < 0.05$ FDR corrected), providing spatio-
365 temporal maps of neural dynamics during object vision (Fig. 3A, red-colored voxels, shown for
366 90, 125 and 160ms; for full time-resolved results see Movie 1). Second, we masked the MEG-
367 fMRI fusion results by the temporal and spatial relationships identified in our MEG-behaviour
368 and fMRI-behaviour analyses respectively. This masking isolates the behaviourally relevant
369 components in the spatio-temporal dynamics of object recognition (Fig. 3A, green-coloured
370 voxels). We found that a subset of the brain activity is behaviourally relevant, spreading rapidly
371 from the occipital pole in anterior direction to high level ventral visual cortex.

372 **5 Discussion**

373 Resolving how the brain translates the sensory stream hitting the retina into behaviour requires
374 the establishment of quantitative relationships between sensory input, neural activity, and
375 behaviour (Ince et al., 2015; de-Wit et al., 2016; Panzeri et al., 2017). Here, we established this
376 link for ecologically valid visual input and behaviour with neural activity in both space and time.

377
378 We suggest the identified behavioural relevant neural activity may play a role in a diverse set of
379 task contexts, as participants performed two different tasks during neuroimaging experiments
380 and behavioural assessments. For behaviour, participants performed a multi-arrangement task
381 judging the perceptual similarity of objects . In MEG and fMRI, participants performed a target
382 detection task which does not involve any active similarity judgments. Because behavioural
383 relevance was established across these very different task contexts, this strongly suggests that
384 the identified representations are behavioural relevant in other tasks as well (Bracci et al.,
385 2017; Kay and Yeatman, 2017). Furthermore, the identified neural activity likely generalizes
386 across subjects, as participants differed across experiments. Thus, the identified neural
387 representations are general and may guide complex human behaviour. Previous studies have
388 identified behaviourally relevant spatiotemporal dynamics of primate brain activity during
389 vision for binary classification tasks (Newsome et al., 1989; Britten et al., 1996; Thorpe et al.,
390 1996; Grill-Spector et al., 2000; VanRullen and Thorpe, 2001; Philiastides and Sajda, 2006;
391 Williams et al., 2007; Ratcliff et al., 2009; Carlson et al., 2013; Ritchie et al., 2015); and for
392 similarity ratings (Op de Beeck et al., 2001; Kayaert et al., 2005; Haushofer et al., 2008; Op de
393 Beeck et al., 2008b p.200; Walther et al., 2009; Mur et al., 2013). Here, we extend those studies
394 in ecological validity by simultaneously using complex arrangement tasks to probe perceived
395 similarity of real-world stimuli, increasing the ecological validity.

396
397 What are the properties of the objects according to which the link between neural activity and
398 behaviour can be established? Two major factors that govern both behaviour and neural
399 activity in high-level ventral visual cortex are category membership (Rosch et al., 1976;
400 Caramazza and Mahon, 2003; Grill-Spector and Malach, 2004; Op de Beeck et al., 2008a) and
401 visual feature similarity (Tanaka, 1996; Op de Beeck et al., 2008a; Yamins et al., 2014). By using
402 a stimulus set where each stimulus was from a different category and by controlling for the
403 effects of supra-ordinate category, we have shown that the brain-behaviour relationship does
404 not solely depend on category membership. This is consistent with the result that neurons in IT
405 carry information about a large set of object properties other than category membership alone
406 (Op de Beeck et al., 2008a; Hong et al., 2016), and suggests that categorisation is only one of
407 many functions of the ventral visual stream.

408

409 To address feature similarity, we investigated whether visual features from a deep neural
410 network (DNN) trained on object categorisation could account for the brain-behavioural link.
411 The DNN did not fully account for this link, which is consistent with the observation that such
412 models do not fully explain activity in the primate visual pathway (Khaligh-Razavi and
413 Kriegeskorte, 2014; Yamins et al., 2014; Güçlü and Gerven, 2015; Cichy et al., 2016a). This might
414 be so because the visual features emerging in the DNN are optimised for the task that the
415 network is trained on, i.e. object categorisation, while categorisation may be only one of the
416 functions of the ventral visual pathway. The fit between brain activity and artificial neural
417 networks might be improved by training DNNs on tasks with higher ecological validity that
418 better capture the richness of human perception than categorisation, such as perceptual
419 similarity arrangements.

420
421 In sum, resolving the neural activity that links sensory experience to behaviour requires
422 differentiating behaviourally relevant neural activity from epiphenomenal activity. Here, by
423 combining brain activity measurements from multiple imaging modalities with an ecologically
424 valid behavioural assessment, we resolved the spatiotemporal dynamics of behaviourally-
425 relevant brain activity for object vision. Our results further strengthen the link between brain
426 activity in ventral visual cortex during object vision and behaviour, and highlight the importance
427 of complex behavioural assessment for human brain mapping.

428 **6 Acknowledgments**

429 This work was funded by the German Research Foundation (DFG, CI241/1-1) to R.M.C. and by
430 the European Research Council (ERC, 680906) to I.C and N.K. MEG and fMRI data were
431 collected at the Athinoula A. Martinos Imaging Center at the McGovern Institute for Brain
432 Research, MIT.

433 **7 References**

- 434 Bracci S, Daniels N, Op de Beeck H (2017) Task Context Overrides Object- and Category-Related
435 Representational Content in the Human Parietal Cortex. *Cereb Cortex* 27:310–321.
- 436 Britten KH, Newsome WT, Shadlen MN, Celebrini S, Movshon JA (1996) A relationship between
437 behavioral choice and the visual responses of neurons in macaque MT. *Vis Neurosci*
438 13:87–100.
- 439 Caramazza A, Mahon BZ (2003) The organization of conceptual knowledge: the evidence from
440 category-specific semantic deficits. *Trends Cogn Sci* 7:354–361.

- 441 Carlson T, Alink A, Tovar D, Kriegeskorte N (2012) The evolving representation of objects in the
442 human brain. *J Vis* 12:272–272.
- 443 Carlson TA, Ritchie JB, Kriegeskorte N, Durvasula S, Ma J (2013) RT for Object Categorization Is
444 Predicted by Representational Distance. *J Cogn Neurosci*:1–11.
- 445 Charest I, Kievit RA, Schmitz TW, Deca D, Kriegeskorte N (2014) Unique semantic space in the
446 brain of each beholder predicts perceived similarity. *Proc Natl Acad Sci*:201402594.
- 447 Cichy RM, Khosla A, Pantazis D, Torralba A, Oliva A (2016a) Comparison of deep neural
448 networks to spatio-temporal cortical dynamics of human visual object recognition
449 reveals hierarchical correspondence. *Sci Rep* 6:27755.
- 450 Cichy RM, Pantazis D, Oliva A (2014) Resolving human object recognition in space and time. *Nat*
451 *Neurosci* 17:455–462.
- 452 Cichy RM, Pantazis D, Oliva A (2016b) Similarity-Based Fusion of MEG and fMRI Reveals Spatio-
453 Temporal Dynamics in Human Cortex During Visual Object Recognition. *Cereb*
454 *Cortex*:bhw135.
- 455 Cichy RM, Teng S (2017) Resolving the neural dynamics of visual and auditory scene processing
456 in the human brain: a methodological approach. *Phil Trans R Soc B* 372:20160108.
- 457 Damasio AR (1990) Category-related recognition defects as a clue to the neural substrates of
458 knowledge. *Trends Neurosci* 13:95–98.
- 459 de-Wit L, Alexander D, Ekroll V, Wagemans J (2016) Is neuroimaging measuring information in
460 the brain? *Psychon Bull Rev* 23:1415–1428.
- 461 DiCarlo JJ, Zoccolan D, Rust NC (2012) How Does the Brain Solve Visual Object Recognition?
462 *Neuron* 73:415–434.
- 463 Grill-Spector K, Kushnir T, Hendler T, Malach R (2000) The dynamics of object-selective
464 activation correlate with recognition performance in humans. *Nat Neurosci* 3:837–843.
- 465 Grill-Spector K, Malach R (2004) The Human Visual Cortex. *Annu Rev Neurosci* 27:649–677.
- 466 Güçlü U, Gerven MAJ van (2015) Deep Neural Networks Reveal a Gradient in the Complexity of
467 Neural Representations across the Ventral Stream. *J Neurosci* 35:10005–10014.
- 468 Hart J Jr, Berndt RS, Caramazza A (1985) Category-specific naming deficit following cerebral
469 infarction. *Nature* 316:439–440.

- 470 Haushofer J, Livingstone MS, Kanwisher N (2008) Multivariate Patterns in Object-Selective
471 Cortex Dissociate Perceptual and Physical Shape Similarity. *PLoS Biol* 6:e187.
- 472 Haynes J-D, Rees G (2005a) Predicting the Stream of Consciousness from Activity in Human
473 Visual Cortex. *Curr Biol* 15:1301–1307.
- 474 Haynes J-D, Rees G (2005b) Predicting the Stream of Consciousness from Activity in Human
475 Visual Cortex. *Curr Biol* 15:1301–1307.
- 476 Haynes J-D, Sakai K, Rees G, Gilbert S, Frith C, Passingham RE (2007) Reading Hidden Intentions
477 in the Human Brain. *Curr Biol* 17:323–328.
- 478 He K, Zhang X, Ren S, Sun J (2015) Deep Residual Learning for Image Recognition.
479 ArXiv151203385 Cs Available at: <http://arxiv.org/abs/1512.03385> [Accessed December
480 12, 2016].
- 481 Heekeren HR, Marrett S, Ungerleider LG (2008) The neural systems that mediate human
482 perceptual decision making. *Nat Rev Neurosci* 9:467–479.
- 483 Hong H, Yamins DLK, Majaj NJ, DiCarlo JJ (2016) Explicit information for category-orthogonal
484 object properties increases along the ventral stream. *Nat Neurosci* 4:613-622
- 485 Ince RAA, Rijsbergen NJ van, Thut G, Rousselet GA, Gross J, Panzeri S, Schyns PG (2015) Tracing
486 the Flow of Perceptual Features in an Algorithmic Brain Network. *Sci Rep* 5:17681.
- 487 Kay KN, Yeatman JD (2017) Bottom-up and top-down computations in word- and face-selective
488 cortex. *eLife* 6:e22341.
- 489 Kayaert G, Irving Biederman, Hans P. Op de Beeck, Rufin Vogels (2005) Tuning for shape
490 dimensions in macaque inferior temporal cortex. *Eur J Neurosci* 22:212–224.
- 491 Khaligh-Razavi S-M, Kriegeskorte N (2014) Deep Supervised, but Not Unsupervised, Models May
492 Explain IT Cortical Representation. *PLoS Comput Biol* 10:e1003915.
- 493 Khosla A, Raju AS, Torralba A, Oliva A (2015) Understanding and Predicting Image Memorability
494 at a Large Scale. In: International Conference on Computer Vision (ICCV).
- 495 Kriegeskorte N (2008) Representational similarity analysis – connecting the branches of systems
496 neuroscience. *Front Syst Neurosci* 2:4.
- 497 Kriegeskorte N, Goebel R, Bandettini P (2006) Information-based functional brain mapping. *Proc*
498 *Natl Acad Sci U S A* 103:3863–3868.

- 499 Kriegeskorte N, Kievit RA (2013) Representational geometry: integrating cognition,
500 computation, and the brain. *Trends Cogn Sci* 17:401–412.
- 501 Kriegeskorte N, Mur M (2012) Inverse MDS: inferring dissimilarity structure from multiple item
502 arrangements. *Front Percept Sci* 3:245.
- 503 Krizhevsky A, Sutskever I, Hinton GE (2012) Imagenet classification with deep convolutional
504 neural networks. In: *Advances in Neural Information Processing Systems*.
- 505 Kubilius J, Bracci S, Beeck HPO de (2016) Deep Neural Networks as a Computational Model for
506 Human Shape Sensitivity. *PLOS Comput Biol* 12:e1004896.
- 507 Mahon BZ, Caramazza A (2009) Concepts and Categories: A Cognitive Neuropsychological
508 Perspective. *Annu Rev Psychol* 60:27–51.
- 509 Martin A, Wiggs CL, Ungerleider LG, Haxby JV (1996) Neural correlates of category-specific
510 knowledge. *Nature* 379:649–652.
- 511 Mur M, Meys M, Bodurka J, Goebel R, Bandettini PA, Kriegeskorte N (2013) Human Object-
512 Similarity Judgments Reflect and Transcend the Primate-IT Object Representation. *Front*
513 *Psychol* 3:456
- 514 Newsome WT, Britten KH, Movshon JA (1989) Neuronal correlates of a perceptual decision.
515 *Nature* 341:52–54.
- 516 Op de Beeck H, Wagemans J, Vogels R (2001) Inferotemporal neurons represent low-
517 dimensional configurations of parameterized shapes. *Nat Neurosci* 4:1244–1252.
- 518 Op de Beeck HP, Haushofer J, Kanwisher NG (2008a) Interpreting fMRI data: maps, modules and
519 dimensions. *Nat Rev Neurosci* 9:123–135.
- 520 Op de Beeck HP, Torfs K, Wagemans J (2008b) Perceived Shape Similarity among Unfamiliar
521 Objects and the Organization of the Human Object Vision Pathway. *J Neurosci*
522 28:10111–10123.
- 523 Panzeri S, Harvey CD, Piasini E, Latham PE, Fellin T (2017) Cracking the Neural Code for Sensory
524 Perception by Combining Statistics, Intervention, and Behavior. *Neuron* 93:491–507.
- 525 Peterson JC, Abbott JT, Griffiths TL (2016) Adapting Deep Network Features to Capture
526 Psychological Representations. *ArXiv160802164 Cs* Available at:
527 <http://arxiv.org/abs/1608.02164> [Accessed January 10, 2017].

- 528 Philiastides MG, Sajda P (2006) Temporal characterization of the neural correlates of perceptual
529 decision making in the human brain. *Cereb Cortex N Y N 1991* 16:509–518.
- 530 Philiastides MG, Sajda P (2007) EEG-Informed fMRI Reveals Spatiotemporal Characteristics of
531 Perceptual Decision Making. *J Neurosci* 27:13082–13091.
- 532 Ratcliff R, Philiastides MG, Sajda P (2009) Quality of evidence for perceptual decision making is
533 indexed by trial-to-trial variability of the EEG. *Proc Natl Acad Sci* 106:6539–6544.
- 534 Ritchie JB, Tovar DA, Carlson TA (2015) Emerging Object Representations in the Visual System
535 Predict Reaction Times for Categorization. *PLoS Comput Biol* 11:e1004316.
- 536 Rosch E, Mervis CB, Gray WD, Johnson DM, Boyes-Braem P (1976) Basic objects in natural
537 categories. *Cognit Psychol* 8:382–439.
- 538 Tadel F, Baillet S, Mosher JC, Pantazis D, Leahy RM (2011) Brainstorm: A User-Friendly
539 Application for MEG/EEG Analysis. *Comput Intell Neurosci* 2011:1–13.
- 540 Tanaka K (1996) Inferotemporal cortex and object vision. *Annu Rev Neurosci* 19:109–139.
- 541 Taulu S, Kajola M, Simola J (2004) Suppression of interference and artifacts by the Signal Space
542 Separation Method. *Brain Topogr* 16:269–275.
- 543 Taulu S, Simola J (2006) Spatiotemporal signal space separation method for rejecting nearby
544 interference in MEG measurements. *Phys Med Biol* 51:1759.
- 545 Thorpe S, Fize D, Marlot C (1996) Speed of processing in the human visual system. *Nature*
546 381:520–522.
- 547 VanRullen R, Thorpe SJ (2001) The time course of visual processing: from early perception to
548 decision-making. *J Cogn Neurosci* 13:454–461.
- 549 Walther DB, Caddigan E, Fei-Fei L, Beck DM (2009) Natural Scene Categories Revealed in
550 Distributed Patterns of Activity in the Human Brain. *J Neurosci* 29:10573–10581.
- 551 Warrington EK, Shallice T (1984) Category specific semantic impairments. *Brain J Neurol* 107 (Pt
552 3):829–854.
- 553 Williams MA, Dang S, Kanwisher NG (2007) Only some spatial patterns of fMRI response are
554 read out in task performance. *Nat Neurosci* 10:685–686.

555 Yamins DLK, Hong H, Cadieu CF, Solomon EA, Seibert D, DiCarlo JJ (2014) Performance-
556 optimized hierarchical models predict neural responses in higher visual cortex. Proc Natl
557 Acad Sci 111:8619–8624.